Received September 26, 2016, accepted October 7, 2016, date of publication November 10, 2016,
date of current version November 28, 2016.

Digital Object Identifier 10.1109/ACCESS.2016.2627623

Unambiguous Tracking Technique Based on Sub-Carrier Pulse Grouping for TMBOC-Modulated Signals in GPS

KEUNHONG CHAE[1], (Student Member, IEEE), SEUNGSOO YOO[2], SUN YONG KIM[2], (Senior Member, IEEE), GYU-IN JEE[2], (Member, IEEE), DONG-JIN YEOM[3], AND SEOKHO YOON[1], (Senior Member, IEEE)

[1]College of Information and Communication Engineering, Sungkyunkwan University, Suwon 16419, South Korea
[2]Department of Electronics Engineering, Konkuk University, Seoul 05029, South Korea
[3]Agency for Defense Development, Daejeon 34186, South Korea

Corresponding author: S. Yoon (syoon@skku.edu)

This work was supported in part by the National GNSS Research Center Program of the Defense Acquisition Program Administration and Agency for Defense Development and in part by the Basic Science Research Program through the National Research Foundation of Korea with funding from the Ministry of Education under Grant 2015R1D1A1A01057327.

ABSTRACT Based on grouping the pulses that compose the sub-carrier of the time-multiplexed binary offset carrier (TMBOC), we present an unambiguous correlation function that has no side-peaks causing the ambiguity in the TMBOC signal tracking, and also, that has a higher degree of the sharpness of the main-peak (DSM) over those of the conventional unambiguous correlation functions. Splitting the pulses composing the TMBOC sub-carrier into 12 groups, and, subsequently, forming the 12 group correlations corresponding to the 12 groups, we investigate the contribution of each of the 12 group correlations to the side peaks and main peak of the TMBOC autocorrelation function. Then, we propose a combining method of the 12 group correlations based on the investigation to remove the side peaks while improving the DSM. Numerical results demonstrate that the proposed unambiguous correlation function not only has no side-peaks, but also has a higher DSM, and, consequently, has a better tracking error performance than those of the conventional unambiguous correlation functions.

INDEX TERMS Ambiguity problem, global positioning system (GPS), side-peak, signal tracking, time-multiplexed binary offset carrier (TMBOC).

I. INTRODUCTION

Recently, the modernization program of the global positioning system (GPS) has adopted the time-multiplexed binary offset carrier (TMBOC) modulation for GPS L1C band [1], [2], since the TMBOC modulation provides a better tracking performance and a higher spectral separation from the binary phased shift keying (BPSK)-modulated signal such as the GPS C/A code signal, when it is compared with the binary offset carrier (BOC) modulation that was used for GPS L1C band [3], [4]. The TMBOC-modulated signal is generated by multiplying a pseudorandom noise (PN) code with the TMBOC sub-carrier comprising $\mathrm{BOC_{sin}}(6,1)$ and $\mathrm{BOC_{sin}}$ (1,1) sub-carriers, where $\mathrm{BOC_{sin}}(x, y)$ denotes the sine-phased BOC signal with the sub-carrier frequency of $x \times 1.023$ MHz and the PN code chip frequency of $y \times 1.023$ MHz for x and y positive real numbers. The modernized GPS L1C band employs the TMBOC (6,1,4/33) signal whose sub-carrier is composed of 4/33 $\mathrm{BOC_{sin}}(6,1)$ sub-carriers and 29/33 $\mathrm{BOC_{sin}}(1,1)$ sub-carriers [5].

The signal tracking is one of the most challenging tasks in the TMBOC-based receiver, since the autocorrelation function of the TMBOC-modulated signal has multiple side-peaks incurring multiple false zero-crossings on the tracking discriminator output. The tracking loop may lock on one of the false zero-crossings, thus leading to a biased tracking measurement, and consequently, a serious pseudo-range estimation error, which is called the problem of ambiguity in tracking.

To overcome the problem, various unambiguous schemes [6]–[14] have been proposed. In [6]–[9], unambiguous discriminator output functions with no false zero-crossings

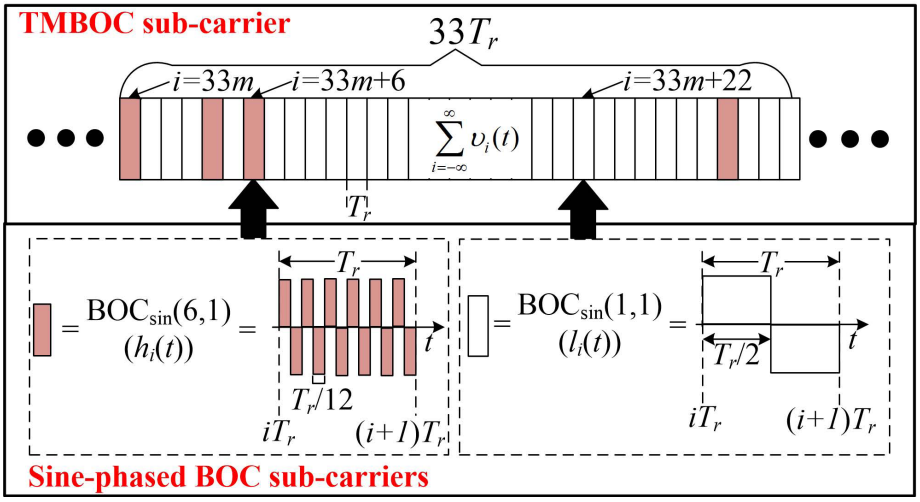

FIGURE 1. The sub-carrier structure of the TMBOC(6,1,4/33) signal.

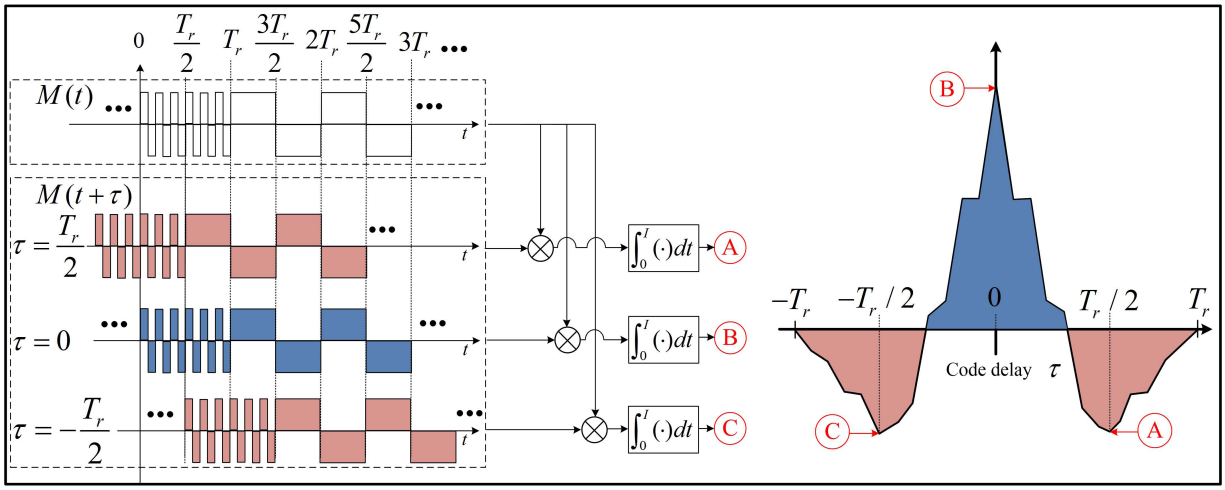

FIGURE 2. The autocorrelation function of the TMBOC(6,1,4/33) signal.

(and thus, with no ambiguity in tracking) were designed based on the cross-correlation between a PN code replica [6] or strobe pulses [7] and the received TMBOC signal, or based on the multiple replicas of the TMBOC autocorrelation function [8], [9]; however, all of the discriminator output functions exhibit a larger tracking error than that of the discriminator output function generated by the traditional TMBOC autocorrelation. In [10]–[14], on the other hand, unambiguous correlation functions with no side-peaks were presented based on the use of various auxiliary signals [10], [11], or based on a combination between the TMBOC autocorrelation function and its modified forms [12]–[14]. Unlike the schemes in [6]–[9] dealing with the false zero-crossings resulting from the side-peaks, these schemes directly remove the side-peaks that are the root cause of the ambiguity, and also, improve the degree of the sharpness of the main-peak (DSM), thus not only removing the ambiguity in tracking completely, but also offering an improvement in tracking error performance over the traditional TMBOC autocorrelation. However, each of the unambiguous correlation functions has a different DSM depending on the cancellation method of the side-peaks used in producing it, and consequently, has a different tracking error performance.

In this paper, thus, we propose a novel cancellation method of the side-peaks to yield an unambiguous correlation function with a higher DSM (and consequently, a better tracking error performance) over those of the conventional unambiguous correlation functions. Splitting the pulses composing the TMBOC sub-carrier into twelve groups, first, we investigate the contribution of each of the twelve group correlations corresponding to the twelve pulse groups to the side-peaks and main-peak, and then, we propose a combining method of the twelve group correlations based on the investigation to remove the side-peaks while improving the DSM. Numerical results confirm that the proposed unambiguous correlation

function has a higher DSM, and consequently, has a better tracking error performance than those of the conventional unambiguous correlation functions. The rest of this paper is organized as follows. Section 2 describes the TMBOC signal model. Section 3 presents the sub-carrier pulse grouping and the associated group correlations, and proposes an unambiguous correlation function with an improved DSM. Section 4 compares the DSMs and tracking error performances of the proposed and conventional unambiguous correlation functions. Finally, Section 5 concludes this paper.

II. TMBOC SIGNAL MODEL

In the TMBOC implementation, 75% and 25% of the total signal power are on the pilot and data components, respectively [2], and, in this paper, we consider the pilot component used for signal synchronization including the tracking. Then, the TMBOC(6,1,4/33) signal $M(t)$ is expressed as [2]

$$M(t) = \sum_{i=-\infty}^{\infty} \sqrt{\rho} L_i \upsilon_i(t), \tag{1}$$

where ρ is the signal power, $L_i \in \{-1, 1\}$ is the ith chip of a PN code with period $I = 10230$ chips, and

$$\upsilon_i(t) = \begin{cases} h_i(t) \text{ for } i = 33m,\ 33m+4,\ 33m+6, \text{ and} \\ \qquad\qquad 33m+29, \text{ for } m \text{ an integer}, \\ l_i(t) \text{ otherwise} \end{cases} \tag{2}$$

is the ith TMBOC(6,1,4/33) sub-carrier with the $\text{BOC}_{\sin}(6,1)$ sub-carrier

$$h_i(t) = \frac{\sin(12\pi(t - iT_r)/T_r)}{|\sin(12\pi(t - iT_r)/T_r)|} \delta_{T_r}(t - iT_r) \tag{3}$$

and the $\text{BOC}_{\sin}(1,1)$ sub-carrier

$$l_i(t) = \frac{\sin(2\pi(t - iT_r)/T_r)}{|\sin(2\pi(t - iT_r)/T_r)|} \delta_{T_r}(t - iT_r), \tag{4}$$

where T_r is the chip period of the PN code and $\delta_{T_r}(t)$ denotes the unit rectangular pulse over $[0, T_r)$. As shown in Fig. 1, the TMBOC(6,1,4/33) sub-carrier has a pattern repeated every $33T_r$ seconds, which comprises 4/33 $\text{BOC}_{\sin}(6,1)$ sub-carriers and 29/33 $\text{BOC}_{\sin}(1,1)$ sub-carriers and will be repeated 310 times since the PN code is 10230 chips long.

III. PROPOSED UNAMBIGUOUS CORRELATION FUNCTION

A. CONTRIBUTION OF THE GROUP CORRELATIONS TO THE AUTOCORRELATION

Fig. 2 depicts how the main-peak and side-peaks of the autocorrelation function of the TMBOC(6,1,4/33) signal are generated, where we can observe that the main-peak is formed when the received and locally generated TMBOC(6,1,4/33) signals are under the in-phase condition (i.e., $\tau = 0$), whereas the side-peaks arise under the opposite-phase condition (i.e., $\tau = \pm T_r/2$). Since the TMBOC(6,1,4/33) sub-carrier consists of multiple pulses

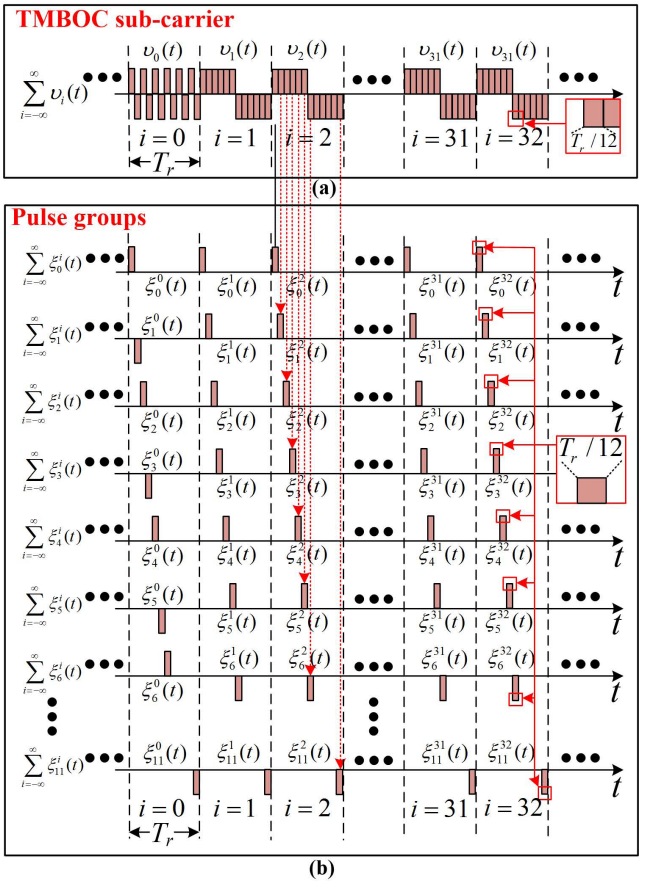

FIGURE 3. (a) The TMBOC(6,1,4/33) sub-carrier model based on pulses with duration $T_r/12$ and (b) twelve pulse groups composing the TMBOC(6,1,4/33) sub-carrier.

as shown in Fig. 1, it would enable us to more clearly understand how the side-peaks and main-peak are generated if we observe the contribution of each of the multiple pulses to the autocorrelation. Each of the multiple pulses has a duration of $T_r/12$ or $T_r/2$ as shown in Fig. 1; yet, the pulse with duration $T_r/2$ can be treated as the sum of the pulses with duration $T_r/12$ having the same amplitude as that of the pulse with duration $T_r/2$, and thus, the TMBOC(6,1,4/33) sub-carrier can be modeled as the sum of the pulses with duration $T_r/12$ as shown in Fig. 3(a). Then, we split the pulses with duration $T_r/12$ into twelve pulse groups as shown in Fig. 3(b), where $\xi_l^i(t)$ denotes the ith pulse of the lth pulse group among the twelve pulse groups (i.e., $l \in \{0, 1, 2, \cdots, 11\}$). Thus, the TMBOC(6,1,4/33) sub-carrier can be expressed as

$$\sum_{i=-\infty}^{\infty} \upsilon_i(t) = \sum_{l=0}^{11} \sum_{i=-\infty}^{\infty} \xi_l^i(t), \tag{5}$$

and the normalized autocorrelation function $\Lambda(\tau)$ of the TMBOC(6,1,4/33) signal is obtained as

$$\Lambda(\tau) = \frac{1}{\rho I} \int_0^I M(t) M(t+\tau) dt$$

$$= \frac{1}{\rho I}\int_0^I M(t)\left[\sum_{i=-\infty}^{\infty}\sqrt{\rho}L_i\upsilon_i(t+\tau)\right]dt$$
$$= \frac{1}{\rho I}\int_0^I M(t)\sum_{l=0}^{11}\left[\sum_{i=-\infty}^{\infty}\sqrt{\rho}L_i\xi_l^i(t+\tau)\right]dt$$
$$= \frac{1}{\rho I}\int_0^I M(t)\sum_{l=0}^{11}M_l(t+\tau)dt$$
$$= \sum_{l=0}^{11}\frac{1}{\rho I}\int_0^I M(t)M_l(t+\tau)dt$$
$$= \sum_{l=0}^{11}\lambda_l(\tau) \quad (6)$$

from (1) and (5), where $M_l(t+\tau) = \sum_{i=-\infty}^{\infty}\sqrt{\rho}L_i\xi_l^i(t+\tau)$ represents the lth component of $M(t+\tau)$ corresponding to the l th pulse group as shown in

$$\sum_{l=0}^{11}M_l(t+\tau) = \sum_{l=0}^{11}\sum_{i=-\infty}^{\infty}\sqrt{\rho}L_i\xi_l^i(t+\tau)$$
$$= \sum_{i=-\infty}^{\infty}\sqrt{\rho}L_i\upsilon_i(t+\tau)$$
$$= M(t+\tau), \quad (7)$$

and similarly, $\lambda_l(\tau) = \frac{1}{\rho I}\int_0^I M(t)M_l(t+\tau)dt$ represents the l th component of the autocorrelation corresponding to the l th pulse group, i.e., $\lambda_l(\tau)$ is the contribution to the autocorrelation of the l th pulse group, which we refer to as the l th group correlation in the sequel.

Fig. 4 shows the twelve group correlations $\{\lambda_l(\tau)\}_{l=0}^{11}$ and their sum, i.e., the autocorrelation, where we can clearly see that all of the group correlations add up at $\tau = 0$ with positive values, forming the main-peak, whereas they add up at $\tau = T_r/2$ with negative values, incurring the side-peaks, and this observation motivates us to implement a novel combination (rather than the simple sum) of the twelve group correlations $\{\lambda_l(\tau)\}_{l=0}^{11}$ that removes the side-peaks while improving the DSM.

B. SIDE-PEAK CANCELLATION AND DSM IMPROVEMENT THROUGH A COMBINATION OF THE GROUP CORRELATIONS

Fig. 5(a) shows that $\lambda_l(\tau)$ and $\lambda_{11-l}(\tau)$ are symmetric around $\tau = 0$, where $l \in \{0, 1, 2, 3, 4, 5\}$, and their product $\lambda_l(\tau)\lambda_{11-l}(\tau) > 0$ when $|\tau| < |\varepsilon_l|$ (i.e., within the main-peak) and $\lambda_l(\tau)\lambda_{11-l}(\tau) \leq 0$ when $|\tau| \geq |\varepsilon_l|$ (i.e., outside the main-peak), where ε_l denotes the zero-crossing of $\lambda_l(\tau)$ closest to $\tau = 0$. This observation implies that the combination $\Gamma[\lambda_l(\tau), \lambda_{11-l}(\tau)] = |\lambda_l| + |\lambda_{11-l}| - |\lambda_l - \lambda_{11-l}|$ can remove the side-peaks while preserving the main-peak, since it is easy to see that

$$\begin{cases} |\alpha| + |\beta| - |\alpha - \beta| > 0, & \text{when } \alpha\beta > 0 \\ |\alpha| + |\beta| - |\alpha - \beta| = 0, & \text{when } \alpha\beta \leq 0, \end{cases} \quad (8)$$

i.e.,$\Gamma[\lambda_l(\tau), \lambda_{11-l}(\tau)]$ yields a positive value due to $\lambda_l(\tau)\lambda_{11-l}(\tau) > 0$ within the main-peak, preserving the main-peak, whereas $\Gamma[\lambda_l(\tau), \lambda_{11-l}(\tau)]$ becomes zero due to $\lambda_l(\tau)\lambda_{11-l}(\tau) \leq 0$ outside the main-peak, removing the side-peaks, which is shown in Fig. 5(b), where we can see that the side-peaks have been removed in each of$\{\Gamma[\lambda_l(\tau), \lambda_{11-l}(\tau)]\}_{l=0}^5$, and thus, we could simply add $\{\Gamma[\lambda_l(\tau), \lambda_{11-l}(\tau)]\}_{l=0}^5$ to yield an unambiguous correlation function; however, the sum of $\{\Gamma[\lambda_l(\tau), \lambda_{11-l}(\tau)]\}_{l=0}^5$ does not give us a sharp main-peak due to $\Gamma[\lambda_2(\tau), \lambda_9(\tau)]$ and $\Gamma[\lambda_3(\tau), \lambda_8(\tau)]$ having two addition peaks similar to the main-peak.

Now, thus, we shift our focus from removing the side-peaks to improving the DSM, with keeping in mind that the DSM improves as the width and height of the main-peak become narrower and higher, respectively. For notational simplicity, we denote $\Gamma[\lambda_l(\tau), \lambda_{11-l}(\tau)]$ by$\chi_l(\tau)$in the rest of this paper. Since$\chi_5(\tau)$has the narrowest width ($T_r/12$) among $\{\chi_l(\tau)\}_{l=0}^5$ and the product of $\chi_5(\tau)$ and each of $\{\chi_l(\tau)\}_{l=0}^5$ has the similar property to that of $\lambda_l(\tau)\lambda_{11-l}(\tau)$ (i.e., the product has a positive and a non-positive values when $|\tau| < |\varepsilon_5|$ and $|\tau| \geq |\varepsilon_5|$,respectively) as shown in Fig. 6(a), we can make the widths of $\{\chi_l(\tau)\}_{l=0}^4$ as narrow as that ($2T_r/24$) of $\chi_5(\tau)$, and also, can increase the heights of $\{\chi_l(\tau)\}_{l=0}^5$ from $4T_r/24$ to $8T_r/24$ by taking $\Gamma[\chi_5(\tau), \chi_l(\tau)]$ for $l \in \{0, 1, 2, 3, 4, 5\}$ as shown in Fig. 6(b). Considering that each of $\{\Gamma[\chi_5(\tau), \chi_l(\tau)]\}_{l=0}^5$ has only a portion of the total correlation power (note that each of $\{\Gamma[\chi_5(\tau), \chi_l(\tau)]\}_{l=0}^5$ is originated from the group correlations composing the auto-correlation), finally, we obtain an unambiguous correlation function $\Psi(\tau)$ having a main-peak with height $2T_r$ and width $2T_r/24$ by adding $\{\Gamma[\chi_5(\tau), \chi_l(\tau)]\}_{l=0}^5$ as shown in Fig. 7, where

$$\Psi(\tau) = \sum_{l=0}^{5}\Gamma[\chi_5(\tau), \chi_l(\tau)]$$
$$= \sum_{l=0}^{5}\Gamma\left[\Gamma[\lambda_5(\tau), \lambda_6(\tau)], \Gamma[\lambda_l(\tau), \lambda_{11-l}(\tau)]\right] \quad (9)$$

and we can see that the proposed correlation function has no side-peaks and has a sharper main-peak (i.e., a higher DSM) compared with the conventional correlation functions, thus allowing us to anticipate that the proposed correlation function offers an improvement in tracking performance over the conventional correlation functions.

C. EXTENSION OF THE PROPOSED SCHEME AND THE ASSOCIATED TRACKING LOOP STRUCTURE

Previously, we treated the pulse with duration $T_r/2$ as the sum of the pulses with duration $T_r/12$ having the same amplitude as that of the pulse with duration $T_r/2$, thus, allowing us to model the TMBOC(6,1,4/33) sub-carrier as the sum of the pulses with duration $T_r/12$. Similarly, the pulse with duration $T_r/12$ can be treated as the sum of the pulses with a shorter duration and the same amplitude as that of the pulse with

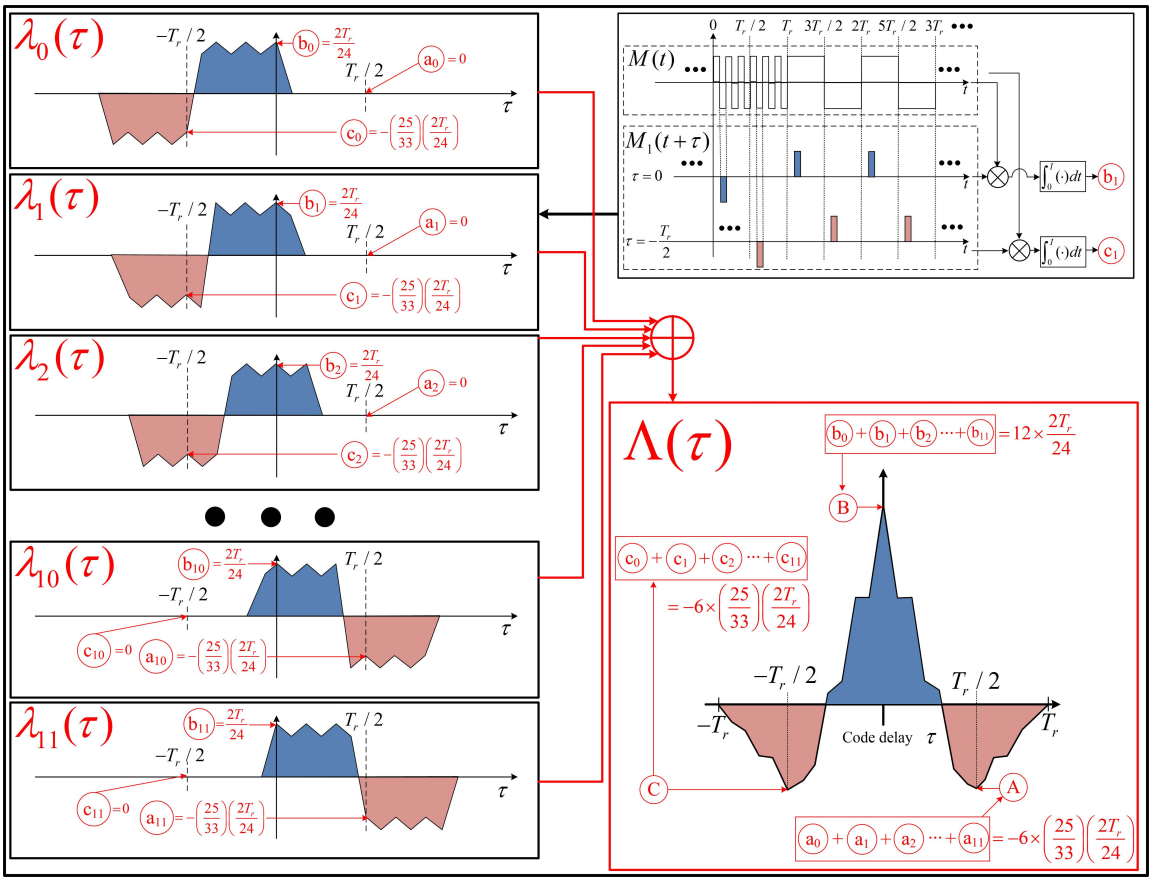

FIGURE 4. Twelve group correlations and the autocorrelation.

duration $T_r/12$: Setting the duration to $T_r/(12q)$, where q is a positive integer, we can model the TMBOC(6,1,4/33) sub-carrier as the sum of the pulses with duration $T_r/(12q)$, and then, can obtain an unambiguous correlation function through the similar steps to those shown in Figs. 5 and 6, which is shown in Fig. 8, where

$$\begin{aligned}\Psi^q(\tau) &= \sum_{l=0}^{6q-1} \Gamma[\chi_{6q-1}(\tau), \chi_l(\tau)] \\ &= \sum_{l=0}^{6q-1} \Gamma\Big[\Gamma[\lambda_{6q-1}(\tau), \lambda_{6q}(\tau)], \\ &\quad \Gamma[\lambda_l(\tau), \lambda_{12q-1-l}(\tau)]\Big], \end{aligned} \tag{10}$$

which is an extended proposed correlation function and reduces to (9) when $q = 1$. As shown in Fig. 8, the height of $\Psi^q(\tau)$ is fixed to $2T_r$ regardless of the value of q, whereas the width $(T_r/(12q))$ of $\Psi^q(\tau)$ becomes narrower as the value of q increases, and thus, the value of the DSM is given by $24q\,(= (2T_r)/(T_r/(12q)))$ and becomes higher as the value of q increases.

Fig. 9 shows the extended proposed correlation function $\Psi^q(\tau)$ when $q = 1,\ 2,\ 3$, and 4 with including the autocorrelation function for a reference, where we can see that $\Psi^4(\tau)$ has the sharpest main-peak as expected, and consequently, the tracking performance is anticipated to be improved as the value of q increases.

Fig. 10 shows the tracking delay lock loop (DLL) structure incorporating the generation process of the extended proposed correlation function given in (10), where Φ denotes the early-late spacing. It should be noted that the pulse group generator and the group correlation generator can be dealt with together by employing a moving sampler as shown in the far-left side of Fig. 10, thus allowing us to use a single correlator instead of $12q$ correlators in each of the early and late branches. The received TMBOC(6,1,4/33) signal is first multiplied with the early and late versions $M(t + \tau \pm \Phi/2)$ of the locally generated TMBOC(6,1,4/33) signal, and then, is correlated and sampled every $T_r/(12q)$ seconds. Subsequently, I/T_r samples are collected and summed in each of the $12q$ branches, yielding the early and late versions $\{\lambda_l(\tau \pm \Phi/2)\}_{l=0}^{12q-1}$ of $12q$ group correlations. Then, the group correlation combiner performs the operation of (10) with $\{\lambda_l(\tau \pm \Phi/2)\}_{l=0}^{12q-1}$ to produce the early and late versions $\Psi^q(\tau \pm \Phi/2)$ of $\Psi^q(\tau)$, and finally, the discriminator output

$$\Delta(\tau) = \left(\Psi^q(\tau + \frac{\Phi}{2})\right)^2 - \left(\Psi^q(\tau - \frac{\Phi}{2})\right)^2 \tag{11}$$

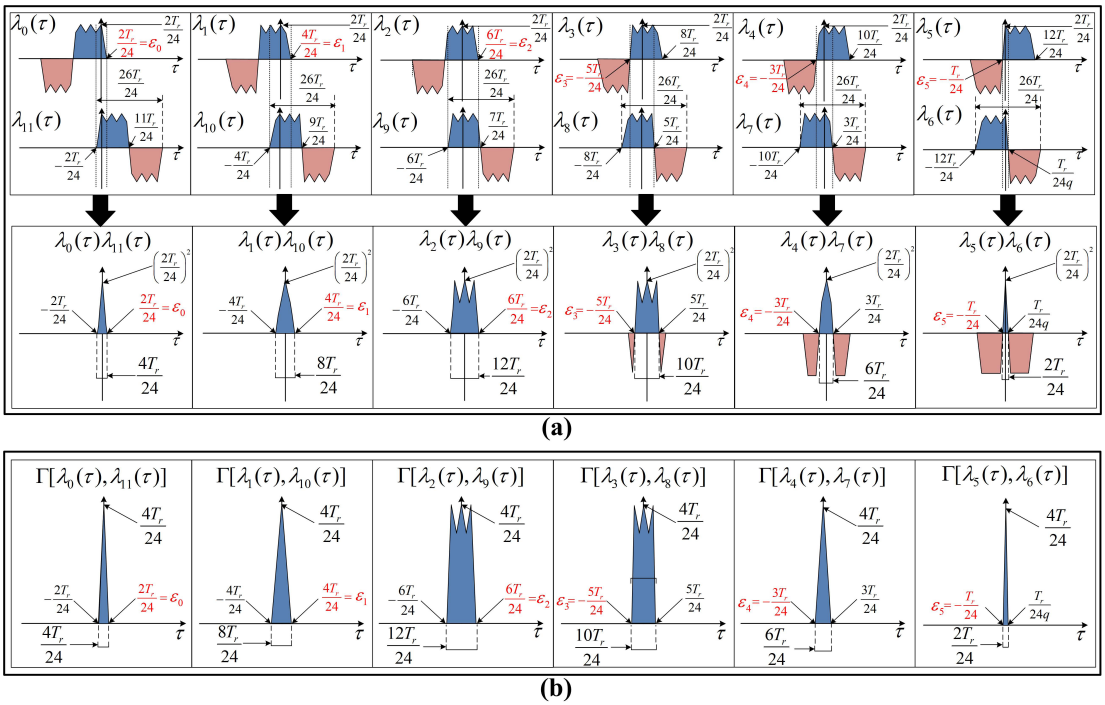

FIGURE 5. (a) The product of two symmetric group correlations and (b) side-peak cancellation through a combination of two symmetric group correlations.

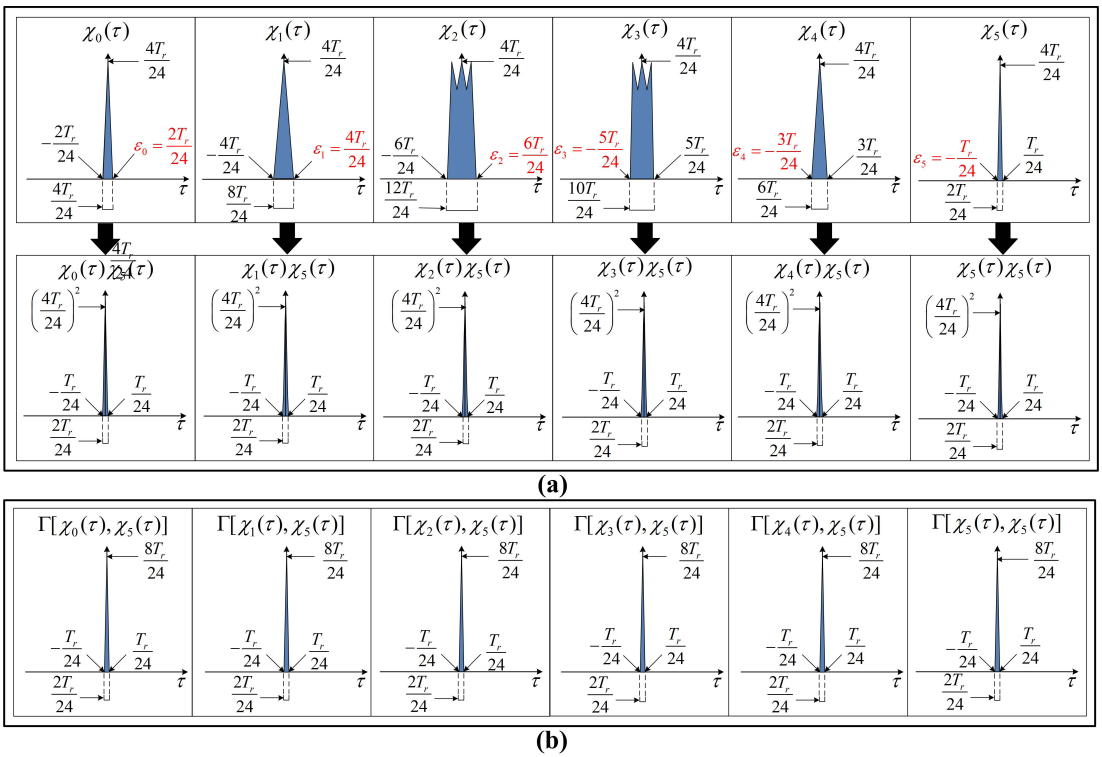

FIGURE 6. (a) The product of $\chi_5(\tau)$ and each of $\{\chi_l(\tau)\}_{l=0}^{5}$ and (b) $\Gamma[\chi_5(\tau), \chi_l(\tau)]$.

is applied to the loop filter to advance or delay the clock of the pulse group generator through the numerically controlled oscillator, which continues until the tracking loop is locked at $\tau = 0$.

IV. NUMERICAL RESULTS

In this section, we show the DSMs of the proposed and conventional correlation functions, and then, compare their tracking performances in terms of the tracking error standard

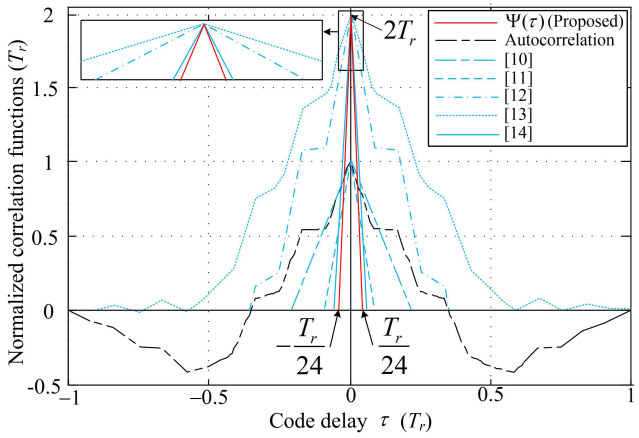

FIGURE 7. The proposed and conventional correlation functions.

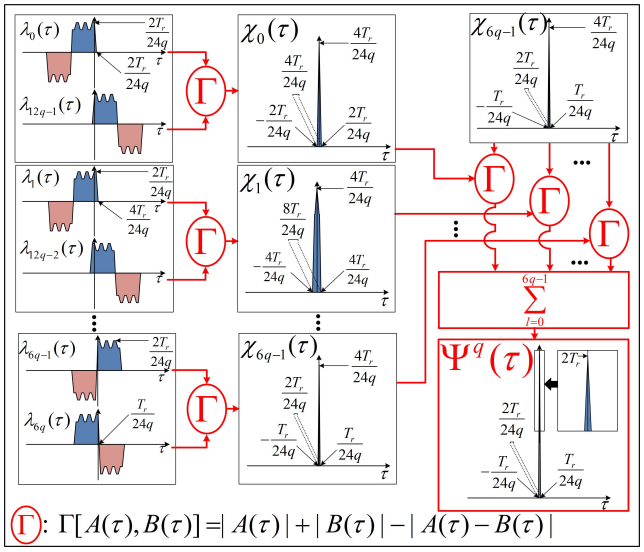

FIGURE 8. The generation process of the extended proposed correlation function.

TABLE 1. Simulation parameters.

Parameter	Value
A	10 ms
T_r^{-1}	1.023 MHz
Ω	1 Hz
Φ	$T_r/96$
q	1, 2, 3, and 4
Number of samples for Monte Carlo simulation	10^5

deviation (TESD) defined as [15]

$$\sqrt{2A\Omega}\frac{V}{D}, \tag{12}$$

where A is the integration time, Ω is the loop filter bandwidth, V is the standard deviation of the discriminator output, and D is the discriminator gain at $\tau = 0$. The parameters used for simulations are shown in Table 1.

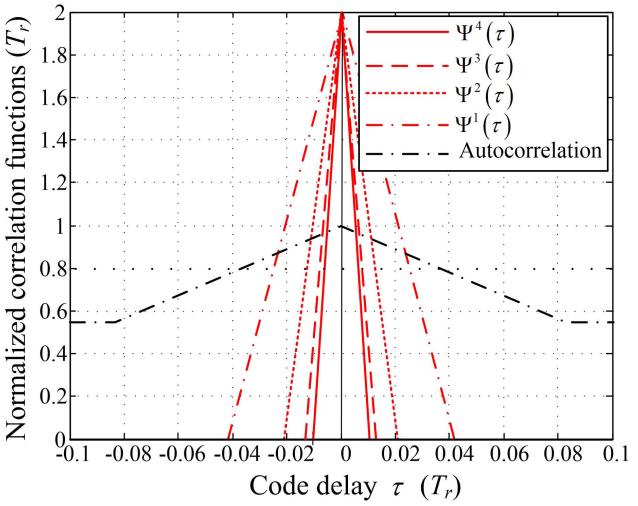

FIGURE 9. The extended proposed correlation functions when $q = 1, 2, 3$ and 4.

TABLE 2. The DSMs of the proposed and conventional correlation functions.

Correlation function	Height (H)	Width (W)	DSM (H/W)
$\Psi^q(\tau)$	$2T_r$	$T_r/12q$	$24q$
[10]	$0.985T_r$	$0.417T_r$	2.362
[11]	T_r	$0.167T_r$	5.988
[12]	$2T_r$	$0.7T_r$	2.857
[13]	$2T_r$	$1.17T_r$	1.709
[14]	$2T_r$	$0.12T_r$	16.667

Table 2 shows the DSMs of the proposed and conventional correlation functions, where H and W denote the height and width of a correlation function employed in tracking, respectively. From Table 2, as expected, the proposed correlation function is seen to have a higher DSM than those of the conventional correlation functions for all values of $q \in \{1, 2, 3, \cdots\}$, which is mainly due to the fact that the width of the proposed correlation function is narrower than those of the conventional correlation functions. On the other hand, the narrower width of the proposed correlation function calls for a higher accuracy in the signal acquisition stage prior to the signal tracking; yet, which can be easily achieved simply by reducing the advancing step size in the acquisition.

Fig. 11(a) shows the TESD performances of the proposed correlation function as a function of q when the values of the carrier to noise ratio (CNR) are 20 dB-Hz, 25 dB-Hz, and 30 dB-Hz, where the CNR is defined as ρ/N_0 with N_0 the noise power spectral density. From the figure, we can observe that the performance improves as the value of q increases; yet, the improvement is saturated eventually for $q \geq 3$.

Fig. 11(b) shows the TESD performances of the proposed and conventional correlation functions as a function of the CNR when $q = 1$ and 3, where the TESD performances of the

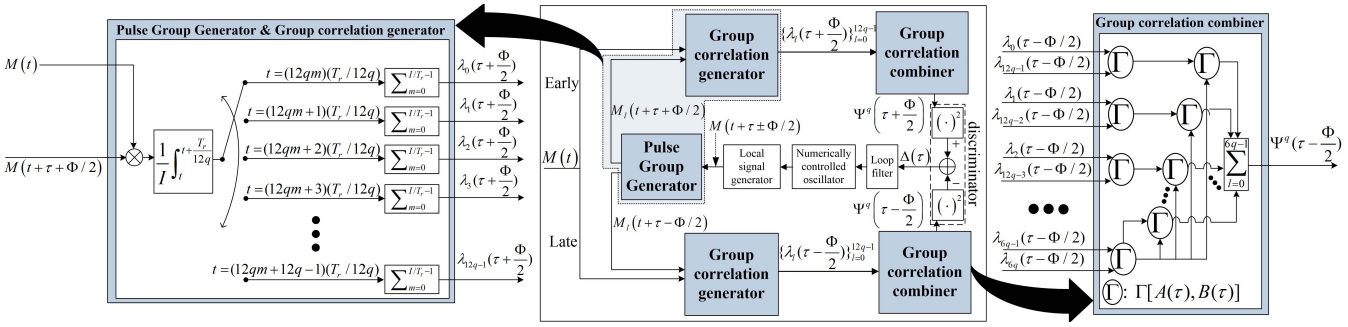

FIGURE 10. The tracking DLL structure incorporating the generation process of the extended proposed correlation function.

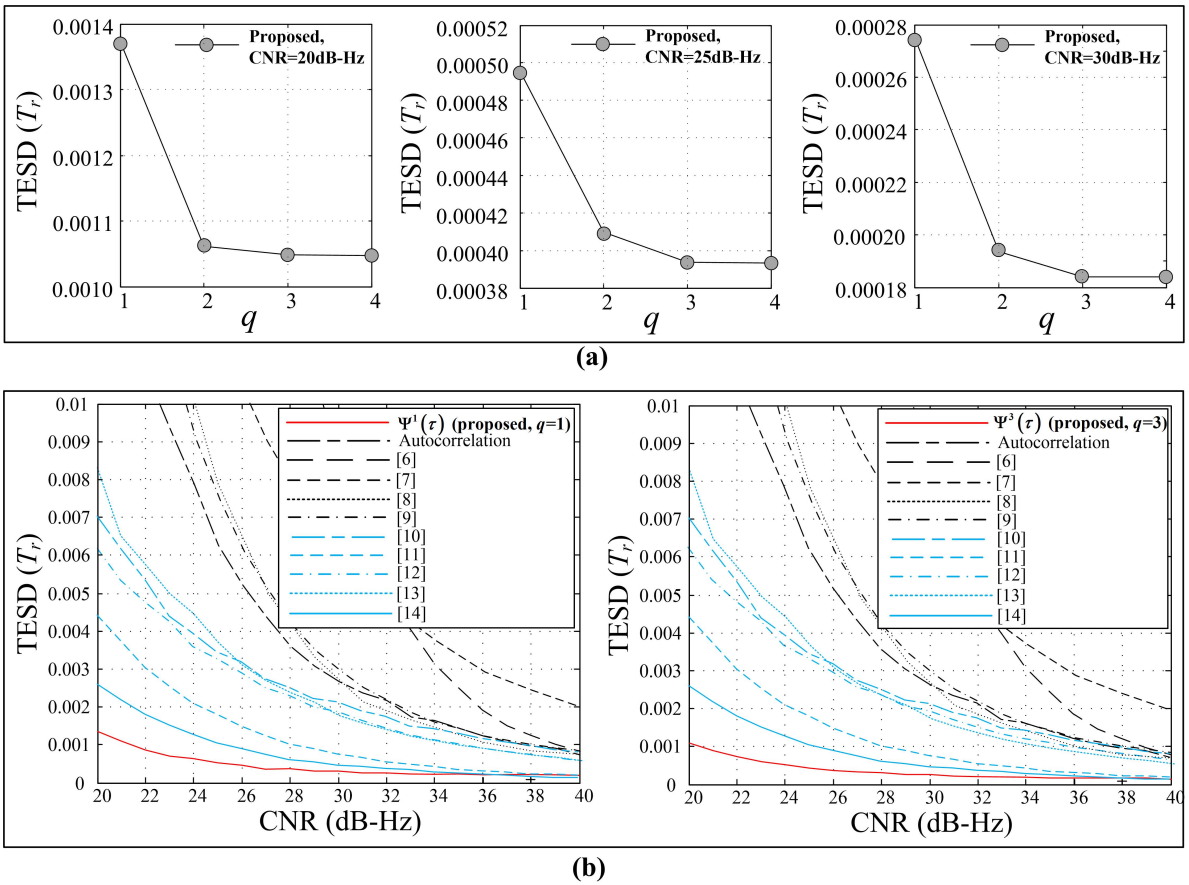

FIGURE 11. (a) TESD performances of the proposed correlation function as a function of q when the CNR is 20 dB-Hz, 25 dB-Hz, and 30 dB-Hz and (b) TESD performances of the proposed and conventional correlation functions as a function of the CNR when $q = 1$ and 3.

autocorrelation function and [6]–[9] based on unambiguous discriminator output functions are also shown for a reference. From the figure, we can clearly see that the proposed correlation function provides a better tracking performance than those of the conventional correlation functions in the CNR range of 20∼40 dB-Hz of practical interest, even when $q = 1$. Specifically, the proposed correlation function gives a performance improvement of more than about 4 dB-Hz, 6 dB-Hz, and 12 dB-Hz over [14], [11], and all of the other conventional schemes, respectively, when $q = 1$, and the difference in performance becomes larger when $q = 3$. In addition, we can see that a correlation function with a higher DSM provides a better signal tracking performance in general, as we expected: The correlation functions corresponding to the three largest DSMs are $\Psi^q(\tau)$, [11], and [14] as shown in Table 2, and they are the three best correlation functions in TESD performance as shown in Fig. 11(b). The trend in performance would remain the same in multipath environments, since the influence of the delayed paths on the first path of interest becomes less significant (i.e., the multipath error becomes smaller) as the DSM increases.

Table 3 shows the complexity comparison of the proposed and conventional correlation functions in terms of the numbers of multiplication, addition, and absolute-value

TABLE 3. The complexities of the proposed and conventional correlation functions.

Correlation function	Number of multiplication operations	Number of Addition operations	Number of Absolute -value operations
$\Psi^q(\tau)$	$2(I/T_r)N_r+2$	$2(I/T_r)N_r+84q-3$	$72q$
[10]	$4(I/T_r)N_r+2$	$4(I/T_r)N_r+3$	6
[11]	$4(I/T_r)N_r+4$	$4(I/T_r)N_r-1$	0
[12]	$2(I/T_r)N_r+2$	$2(I/T_r)N_r+1$	2
[13]	$2(I/T_r)N_r+2$	$2(I/T_r)N_r+1$	0
[14]	$4(I/T_r)N_r+6$	$4(I/T_r)N_r+3$	6

operations, where N_r is the number of samples within the chip duration T_r of the PN code. Considering that the period of the PN code used for TMBOC(6,1,4/33) signal is very long (i.e., $I/T_r = 10230 \gg 1$), we can see that the proposed correlation function requires almost the same number of multiplication and addition operations as those of [12] and [13], and only about half the number of multiplication and addition operations of [10], [11], and [14]. Yet, the proposed correlation function requires more number of absolute-value operations than those of the conventional correlation functions, and thus, it would be interesting to develop a modified version of the proposed correlation function with a lower complexity in a sequel paper.

Finally, let us add a brief discussion on the physical meaning of the parameter q and on how a designer can choose the best value of q. From Fig. 3 and Section III, we can see that the value of q determines the duration of a unit pulse composing the pulse groups (specifically, the duration is given by $T_r/(12q)$), and since the proposed correlation function can be considered as a constructive combination of the unit pulses, its width is proportional to the duration of the unit pulse. Thus, a larger value of q results in a narrower duration of the unit pulse, and eventually, a narrower width of the proposed correlation function, making the DSM and tracking performance of the proposed correlation function higher and better, respectively. Yet, a larger value of q involves an increase in implementation complexity as shown in Table 3, and also, does not provide a significant improvement in performance when it exceeds a specific value as shown in Fig. 11. Thus, the best value of q can be considered to be a specific value resulting in a saturation in performance improvement. From Fig. 11 and Table 3, for example, we can conclude that $q = 3$ is the best choice for the proposed correlation function.

V. CONCLUSIONS

In this paper, we have proposed an unambiguous correlation function with an improved DSM based on the TMBOC sub-carrier pulse grouping for the TMBOC(6,1,4/33) signal tracking. Observing that the correlation side-peaks and main-peak result from the sum of the twelve group correlations corresponding to the twelve TMBOC sub-carrier pulse groups, we have presented a new combining method of the twelve group correlations to replace the simple sum of them, which has been found to not only remove the side-peaks, but also improve the DSM. In addition, we have shown that the higher DSM is achieved by splitting the TMBOC sub-carrier pulses into more than twelve groups, and have introduced a tunable parameter for adjusting the number of the groups. It has been confirmed from the numerical results that the proposed unambiguous correlation function has a higher DSM (and consequently, a better tracking error performance) than the conventional unambiguous correlation functions, and its tracking performance becomes better as the value of the tunable parameter increases, at the cost of an increased implementation complexity.

REFERENCES

[1] J. W. Betz *et al.*, "Description of the L1C Signal," in *Proc. ION GNSS*, Fort Worth, TX, USA, 2006, pp. 2080–2091.

[2] V. U. Zavorotny, S. Gleason, E. Cardellach, and A. Camps, "Tutorial on remote sensing using GNSS bistatic radar of opportunity," *IEEE Geosci. Remote Sens. Mag.*, vol. 2, no. 4, pp. 8–45, Dec. 2014.

[3] G. W. Hein *et al.*, "MBOC: The new optimized spreading modulation recommended for GALILEO L1 OS and GPS L1C," in *Proc. IEEE/ION PLANS*, San Diego, CA, USA, Apr. 2006, pp. 884–892.

[4] S. Zitouni, D. Chikouche, and K. Rouabah, "Common GPS/Galileo signals: MBOC VS BOC (1, 1) performance comparison," in *Proc. Int. Workshop Syst., Signal Process. Appl. (WoSSPA)*, Zéralda, Algeria, 2013, pp. 510–514.

[5] O. Julien, C. Macabiau, J. L. Issler, and L. Ries, "1-bit processing of composite BOC (CBOC) signals and extension to time-multiplexed BOC (TMBOC) signals," in *Proc. ION NTM*, San Diego, CA, USA, 2007, pp. 227–239.

[6] A. G. Dempster and J. Wu, "Code discriminator for multiplexed binary offset carrier modulated signals," *Electron. Lett.*, vol. 44, no. 5, pp. 384–385, Feb. 2008.

[7] Z. Liu, J. Pang, Y. Liu, and F. Wang, "Double strobe technique for unambiguous tracking of TMBOC modulated signal in GPS," *IEEE Signal Process. Lett.*, vol. 22, no. 12, pp. 2204–2208, Dec. 2015.

[8] D. W. Lim, D. J. Cho, H. H. Choi, and S. J. Lee, "A simple and efficient code discriminator for a MBOC signal tracking," *IEEE Commun. Lett.*, vol. 17, no. 6, pp. 1088–1091, Jun. 2013.

[9] J. Ren, S. Zhou, W. Jia, and M. Yao, "Non-coherent unambiguous tracking method for composite binary offset carrier modulated signals based on S-curve shaping technique," *IEEE Commun. Lett.*, vol. 17, no. 8, pp. 1540–1543, Aug. 2013.

[10] Z. Yao, M. Lu, and Z. Feng, "Unambiguous technique for multiplexed binary offset carrier modulated signals tracking," *IEEE Signal Process. Lett.*, vol. 16, no. 7, pp. 608–611, Jul. 2009.

[11] D. Xu, M. Liu, and F. Shen, "Ambiguity mitigating technique for multiplexed binary carrier signal tracking," *IEEE Commun. Lett.*, vol. 17, no. 11, pp. 2021–2024, Nov. 2013.

[12] Z. Yanling, H. Xiulin, and T. Zuping, "Unambiguous tracking technique for Sin-BOC(1,1) and MBOC(6,1,1/11) signals," in *Proc. Int. Conf. Future Comput. Commun. (ICFCC)*, Wuhan, China, 2010, pp. 188–190.

[13] K. Rouabah, M. Flissi, S. Attia, and D. Chikouche, "Unambiguous multipath mitigation technique for BOC (n, n) and MBOC-modulated GNSS signals," *Int. J. Antennas Propag.*, vol. 2012, p. 13, Jul. 2012, Article. no. 895390.

[14] H. Li and C. Yang, "Unambiguous receiving technique for multiplexed binary offset carrier signal," in *Proc. Int. Conf. Wireless Commun. Signal Process. (WCSP)*, Hefei, China, 2014, pp. 1–5.

[15] A. J. Van Dierendonck, P. Fenton, and T. Ford, "Theory and performance of narrow correlator spacing in a GPS receiver," *J. Inst. Navigat.*, vol. 39, no. 3, pp. 265–283, Sep. 1992.

KEUNHONG CHAE (S'14) received the B.S.E. degree in information and communication engineering from Sungkyunkwan University, Suwon, South Korea, in 2014, where he is currently pursuing the Ph.D. degree with the College of Information and Communication Engineering. His research interests include mobile communications, satellite communications, and detection and estimation theory.

SEUNGSOO YOO received the Ph.D. degree in electronics engineering from Konkuk University, Seoul, South Korea. Since 2013, he has been with the College of Information and Communications, Konkuk University, where he is currently an Assistant Professor. His research interests include anti-jamming techniques for global navigation satellite system and statistical signal processing.

SUN YONG KIM (SM'04) received the Ph.D. degree in electrical engineering from the Korea Advanced Institute of Science and Technology, Daejeon, South Korea. Since 1995, he has been with the Department of Electronics Engineering, Konkuk University, Seoul, South Korea, where he is currently a Professor. His research interests include mobile communications, detection and estimation theory, and statistical signal processing.

GYU-IN JEE (S'82–M'90) received the Ph.D. degree in systems engineering from Case Western Reserve University, Cleveland, OH, USA. He is currently a Professor with the Department of Electronics Engineering, Konkuk University, Seoul, South Korea. His research interests include integrated vehicle navigation system, GNSS receiver signal processing, and precise localization system for autonomous vehicle.

DONG-JIN YEOM received the B.S. and M.S. degrees in electronics engineering from Chungnam National University, South Korea, in 1991 and 1993, respectively. Since 1993, he has been with the Agency for Defense Development in RF Systems Technology Directorate. His research interests are in radar signal processing and active radar array.

SEOKHO YOON (S'99–M'02–SM'07) received the B.S.E. (*s*umma cum laude), M.S.E., and Ph.D. degrees in electrical engineering from the Korea Advanced Institute of Science and Technology, Daejeon, South Korea, in 1997, 1999, and 2002, respectively. In 2002, he was with the Department of Electrical Engineering and Computer Sciences, Massachusetts Institute of Technology, Cambridge, MA, USA, and from 2002 to 2003, he was with the Department of Electrical Engineering, Harvard University, Cambridge, as a Post-Doctoral Research Fellow. In 2003, he joined the College of Information and Communication Engineering, Sungkyunkwan University, Suwon, South Korea, where he is currently a Professor. His research interests include spread spectrum and OFDM systems, mobile/satellite communications, detection and estimation theory, and statistical signal processing. He is a member of the Institute of Electronics, Information and Communication Engineers, and a Lifetime Member of the Korean Institute of Communication Sciences.